Project title:	Review of surface parameterisation method for shape optimisation of transonic aerofoil for commercial transport aircraft
Student:	Alejandro González Pérez
Advisor:	Professor Christian B. Allen

Executive summary

Aerodynamic shape optimisation is a complex discipline that involves multiple stages. Firstly, the optimisation problem must be formulated mathematically by specifying an objective function and set of constraints that correctly represent the physical problem. A suitable parameterisation scheme must then be chosen to ensure good coverage of the design space is attained, and an adequate optimisation algorithm must be identified to minimise the aforementioned objective function. Said optimiser must be coupled to a flow solver to perform the corresponding objective function evaluations.

A typical transonic transport aircraft shape optimisation problem has been proposed and a novel surface parameterisation method based on Singular Value Decomposition of a training library of aerofoils has been investigated as a potential candidate. A formulation based on Radial Basis Functions has been replicated to provide a link between surface deformations and deformations of the volumetric CFD mesh used for performing the objective functions evaluations.

The main issues arising from a typical aerodynamic optimisation exercise have been reviewed and possible remedies discussed for some. A gradient-based optimiser has been proposed as a suitable algorithm to perform an aerodynamic optimisation to solve the described optimisation problem as an extension to this project.

1 Introduction

1.1 Problem description

The application of numerical methods to aerodynamic shape optimisation (ASO) has proved a fundamental problem for aerodynamicists since the usage of computational fluid dynamics (CFD) became the standard for aerofoil design in the 1970s [1]. Inextricably intertwined to the availability of computer power, the future of CFD is threatened by the recent deceleration in the rate of increase of processing power [2]. The development of efficacious, robust methods for ASO is thus imperative for the future of the aerodynamic design industry.

1.2 Background

ASO is a complex process that comprises of several different steps. Firstly, the optimisation problem must be described mathematically. A typical optimisation problem is of the form [3, 4]:

$$\begin{aligned} &\text{minimise}: && J(\boldsymbol{\alpha}) && \text{(objective function)} \\ &\text{subject to}: && \boldsymbol{g}(\boldsymbol{\alpha}) \leq 0 && \text{(inequality constraint)} \\ &&& \boldsymbol{h}(\boldsymbol{\alpha}) = 0 && \text{(equality constraint)} \\ &&& \alpha_i^l \leq \alpha_i \leq \alpha_i^u && \text{(side constraints)} \end{aligned} \tag{1}$$

where $\boldsymbol{\alpha} = \{\alpha_1, ..., \alpha_i, ..., \alpha_D\}$ is the vector of design variables. Side constrains are sometimes included within the inequality constraints, but it can also be convenient to leave them aside – for instance, they could represent the structural sizing requirements for an ASO problem.

A surface parameterisation scheme must then be chosen to obtain a set of design variables $\boldsymbol{\alpha}$. The strong dependence of the optimisation problem on $\boldsymbol{\alpha}$ – as evidenced by Eq. (1) – results in the necessity to implement an efficient geometric parameterisation method that reduces the cost of the optimisation process but retains a good coverage of the design space [5].

1.3 Procedure

In order to provide an effective comparison of different shape parameterisation methods, a relevant aerodynamic design exercise has been considered. The design specification has been taken from Buckley *et al.* [6] and consists in the design of an optimum aerofoil for use at the mean aerodynamic chord (MAC) of a $100,000\,\mathrm{lb}$ transonic aeroplane (maximum cruise Mach of 0.88) with a wing area of $1,000\,\mathrm{ft}^2$ and a wing sweep of $35°$. The target thickness-to-chord ratio was set to 0.12.

A training library consisting of 1300 aerofoils was used to provide a definition of the design space. The different methods of parameterising the library considered were categorised as constructive or deformative depending on how they interacted with the volumetric mesh used for the CFD calculations on each iteration of the optimisation algorithm.

The required optimisation problem was then formulated mathematically by deriving a suitable objective function that represented the physical problem adequately. The challenge of finding a suitable optimisation algorithm was identified and its solution proposed as an extension to this project.

2 Aims and Objectives

The aim of this project was to study the feasibility of applying a novel surface parameterisation scheme to perform an aerodynamic shape optimisation of a transonic aerofoil for application in a transport commercial aircraft, and to provide a comparison with respect to other available surface parameterisation schemes.

1. Identify potential aerodynamic design requirements for a typical commercial transport aircraft, and derive the corresponding objective function to formulate the shape optimisation problem.

2. Recognise alternative surface parameterisation methods applicable to the ASO of a transonic aerofoil for a commercial transport aircraft, and provide a comparison with the SVD method utilised.

3. Identify an adequate optimisation algorithm to perform the aimed ASO based on the available computational power, and hence identify an effi-

cient method to couple the optimisation algorithm to a suitable flow solver.

3 Training library

A training library of 1300 aerofoils provided by the University of Bristol has been utilised for this project. The library had been extracted from the UIUC Airfoil Coordinates Database* and subsequently normalised to a length of 1 MAC by fixing leading edge and trailing edge at points $[0, 0]$ and $[1, 0]$, respectively. To ensure a constant geometrical distribution for all aerofoils, these had been parameterised using a half-cosine squared geometrical distribution, as detailed in Appendix A of Masters *et al.* [7].

The UIUC library consists of numerous aerofoils of varied expected performance for the studied design problem. It is anticipated that the quality of the aerofoils derived from the extracted design variables be limited to the quality of the originating library. Reducing the size of the working library would decrease the dimensionality of the resulting design space, and hence the modality of the search space [8]. Hence, a method of efficiently filtering the working library without impacting performance needs be identified.

The Korn technology factor κ [9] has been utilised in this project to effectively rank the expected performance of the aerofoil library in a transonic regime. Typical values of κ - Eq. (2) - are 0.95 for supercritical aerofoils and 0.87 for conventional aerofoils [9, 10]. Mason [10] shows that these values agree with experimental data from NASA [11] and Shevell [12] for values of the lift coefficient of up to $C_L = 0.7$, and for both supercritical and traditional aerofoil sections except older sections with smaller thickness-to-chord ratios t/c.

$$\kappa = M_{\mathrm{DD}} + \frac{C_L}{10} + \frac{t}{c} \tag{2}$$

The drag divergence Mach number M_{DD} is defined as the point at which the gradient of the drag-to-Mach curve reaches the value 0.1 - as defined in Eq. (3) - for a fixed value of C_L. This value of the Mach number is marginally above the critical value M_{cr}, and is associated to a considerable extension of supersonic flow on the top surface of the aerofoil that results in a shockwave. The critical Mach – and hence the drag divergence Mach – can be delayed by reducing the aerofoil thickness [13]. The Korn technology factor identifies the relationship between drag divergence and the corresponding lift and aerofoil thickness, and therefore considers the gap between M_{cr} and M_{DD} to assess technology integration at transonic conditions.

$$\left.\frac{\partial C_D}{\partial M}\right|_{M_{\mathrm{DD}}} = 0.1 \tag{3}$$

M_{DD} was estimated for each aerofoil at the design lift coefficient of $C_L = 0.74$†. Prior to each evaluation of the drag gradient, the required angle of attack for the design lift was estimated using a secant-based root-finding algorithm with an initial guess taken from thin aerofoil theory. Aerofoils incapable of meeting the lift coefficient requirements before drag divergence were filtered out. The drag gradient was then estimated using a central finite-difference approximation, and a bisection-based root finding algorithm used to solve Eq 3.

4 Parameterisation schemes

In order to provide a robust optimisation method, good coverage of the design space must be achieved by the chosen parameterisation scheme, which can be classified as constructive or deformative based on its interaction with the CFD mesh used.

4.1 Deformative schemes

Deformative methods generate new aerofoils by directly updating the points in the working mesh. The shape parameters are hence deformations of the initial aerofoil, which makes the methods independent of the initial aerofoil selection. It also makes them comparatively more flexible as it is generally easier to match deformations to the de-

*Aerofoil database available online at https://m-selig.ae.illinois.edu/ads/coord_database.html.

†Justification for the chosen C_L value, and information on the flow solver and mesh used are presented in Sec. 5

sired change in shape, but at the expense of not guaranteeing smoothness of the resulting surfaces.

4.1.1 Singular Value Decomposition

Given a rectangular matrix X, its Singular Value Decomposition (SVD) is defined as the following decomposition:

$$X = U\boldsymbol{\Sigma}V^T \tag{4}$$

where U and V are unitary matrices, and $\boldsymbol{\Sigma}$ is a diagonal matrix containing the singular values of X [14]. The dimensionality of the SVD can be reduced by discarding the smallest singular values, and hence eliminating the corresponding columns from U and V. Typically, a number of singular values is kept that conserves at least 90% of the total energy in Σ [15], where energy is defined as the sum of the squares of the singular values (*i.e.* the sum of the eigenvalues of X).

The usage of SVD for extraction of modal variables was first presented by Poole *et al.* [16]. This approach can be formulated in either a constructive fashion, by taking X to be the library matrix containing the coordinate locations for all aerofoils in the library; or in a deformative manner, by taking X to be a matrix containing all the possible deformations between corresponding surface points on the library aerofoils. In the latter case, new working shapes are obtained by summing a linear combination of the resulting modal shapes (U^i) to the previous shape, where the linear coefficients are the design variables themselves (5).

$$X \to X + \sum_{i=1}^{D} \alpha_i U^i \tag{5}$$

4.1.2 Mesh deformation

The main strength of deformative schemes resides in the suppression of the need to generate a new aerodynamic mesh for each modification of the working geometry, which results in a reduction of the overall computational cost of the optimisation process. A method of efficiently coupling aerofoil shape deformations to aerodynamic mesh deformations must then be envisaged. Most mesh deformation methods rely on mesh connectivity (*e.g.* spring-analogy [17] and linear elastic analogy [18]). This is not necessarily an issue for optimisation problems when simple mesh geometries are used (as is the case of the O-mesh chosen for this project), but can prove problematic for multi-mesh optimisation problems where connectivity is not evident.

For this project, a method based on radial Radial Basis Functions (RBFs) has been selected to link deformations of a set of N_{CP} control points to corresponding deformations of the aerodynamic surface and mesh points. The usage of RBFs for interpolation of scattered data was first presented by Wendland [19] and Buhmann [20], and its application to mesh motion as implemented in this project, by Rendall and Allen [21].

RBFs allow to update the positions of any spacial points by evaluating the weighted deformations of a set of control points. The main advantage of this method is that it is utterly mesh-independent as it does not require connectivity data, whilst still maintaining mesh quality after deformations [21].

Control points can be placed both on and off-surface – on-surface points have been chosen here to provide direct linking between surface deformations and control point deformations. Masters *et al.* [7] showed that between 20 to 25 control points are enough to represent an exhaustive aerofoil training library to manufacturing tolerance, and therefore 24 control points have been utilised here.

A typical RBF interpolation is of the form:

$$\Delta\boldsymbol{x}(\boldsymbol{x}) = \sum_{i=1}^{N_{\mathrm{CP}}} \gamma_i \phi\left(||\boldsymbol{x} - \boldsymbol{x_i}||\right) + p(\boldsymbol{x}) \tag{6}$$

where $r_i = ||\boldsymbol{x} - \boldsymbol{x_i}||$ is the radial distance to the i-th control point as defined by the Euclidean norm $||\cdot||$; γ_i is the corresponding control point weighting coefficient; $\phi(r)$ is the corresponding evaluation of the chosen RBF, and $p(\boldsymbol{x})$ is a polynomial term. This polynomial term is required to recover translation and rotations of the design shape [22], and has therefore been omitted as unnecessary for the normalised aerofoil shapes studied.

Determination of the dependence coefficient vector γ is achieved by forcing an exact recovery of the RBF values at each control point.

$$\boldsymbol{x_{CP}} = C_{\mathrm{CP}}\,\gamma \tag{7}$$

where C_{CP} is the global control point influence matrix and can be calculated as shown in Eq. (8). The obtention of the model coefficients thus reduces to solving a system of equations given by a positive definite matrix, a simple problem solved by a Cholesky decomposition and for which substantial work in efficiency improvement has been carried out globally [23].

$$C_{\mathrm{CP}} = \begin{pmatrix} \phi_{11} & \cdots & \phi_{1N_{\mathrm{CP}}} \\ \vdots & \ddots & \vdots \\ \phi_{N_{\mathrm{CP}}1} & \cdots & \phi_{N_{\mathrm{CP}}N_{\mathrm{CP}}} \end{pmatrix} \tag{8}$$

Different types of functions can be used to perform the required interpolation: global, local and compact functions. Local and compact functions are preferred when working with deformations to ensure these are localised in a region near the working aerofoil [24]. Compact functions have the additional property of limiting transformed deformations to a certain area defined by a support radius R – decaying to zero at any points further afield.

Larger values of the support radius result in a smoother function and hence improved interpolation quality, however they have a negative impact in matrix conditioning (the matrix sensitivity to small perturbations). Morris, Allen and Rendall [25] found that Wendland's C^2 function (Eq. 9) provided the best tradeoff between deformation quality and matrix conditioning of all of Wendland's compact functions [19], and therefore is used here.

$$\phi(r) = \begin{cases} (1-r)^4 \cdot (4r-1) & \text{if } r < 1 \\ 0 & \text{otherwise} \end{cases} \tag{9}$$

It must be noted that the value of r in Eq. (9) has been scaled down by a factor of R^{-1} to define a unitary hypersphere representing the zone of influence of the control point deformations. Rendall and Allen [26] suggest that R must be several factors higher than the biggest motion of any surface point, and thus a support radius of 1 MAC has been chosen.

4.2 Constructive schemes

Constructive schemes generate new aerofoils by defining the shapes directly using a set of design variables, and are therefore inextricably intertwined to the working surface - prior to starting the optimisation process an expression for the initial aerofoil must be derived. They tend to be more intuitive than deformative methods, as design variables can be chosen to represent characteristic aspects of the aerofoil, which makes them easier to integrate in the aircraft design stages.

4.2.1 CST Method

The Class function/Shape function Transformation (CST) method [27, 28] allows the parameterisation of aerofoils to the desired tolerance using a small number of design variables. For a unit-chord normalised aerofoil with a round nose and sharp trailing edge, the upper and lower aerofoil surfaces can be parameterised as:

$$z(x) = \left[\sqrt{x}\,(1-x)\right] \cdot S(x) \tag{10}$$

where $S(x)$ is a unit "shape function" that represents the key geometrical features of the represented aerofoil, or design variables. Kulfan and Bussoletti [27] proved that the unit shape function can be decomposed to the summation of an arbitrary number of component shape aerofoils using Bernstein polynomials - as shown in Eq. (11).

$$S(x) = \sum_{i=0}^{n} \alpha_i x^i (1-x)^{n-i} + \alpha_{n+1}\sqrt{x}(1-x)^{n-0.5} \tag{11}$$

The term on $n+1$ was proposed as an *a posteriori* addition by Kulfan to remedy the lack of a linear term near the leading edge that resulted in poor convergence for certain aerofoil geometries [29].

Kulfan showed that adding this term would result in a reduction in the number of required design variables, with additional improvement for the parameterisation of transonic and supersonic aerofoils.

The need to add said term to improve robustness of the CST method clearly illustrates the main weaknesses of most constructive methods. On the one hand, complex curvatures (or infinite slopes) cannot be easily parameterised and require the usage of more design variables. On the other hand, the higher order polynomials resulting from the increase in design variables can induce undesired surface oscillations, especially for small variable changes, thus limiting the potential for optimisation.

5 Optimisation framework

5.1 Mathematical formulation

The multiplicity of operating conditions of a typical civil aircraft mission results in a complex ASO problem that is multi-objective in nature. Most optimisation publications ignore off-design conditions and focus on on-design, which is generally sufficient to prove the validity of a given optimisation algorithm, but fails to provide an accurate representation of the usefulness of ASO in a real design exercise [30]. Buckley *et al.* [6, 31] tackles this issue by performing multipoint design optimisation including a range of off-design conditions. Albeit resulting in a boost in overall robustness, the cost of multipoint optimisation may well prove prohibitive, as computational cost increases linearly with the number of design points.

A similar issue arises when considering single-point optimisation of transonic aerofoils, where the resulting shapes tend to be supercritical and produce shock-free solutions. These solutions are isolated and result in relatively strong shocks when the flow Mach number is disturbed from the design condition [32–34], thus compromising the overall performance of the optimisation. Poole *et al.* [35] proposed a solution to this problem considering de Breguet range optimisation – instead of the classical drag minimisation exercise – and including an induced drag coefficient κ to the de Breguet parameter to model the physical tradeoff between speed, lift production and drag. This optimisation case required constraining the problem based on a measure of non-dimensional lift, and setting the Mach number as a new design variable to allow it to change alongside lift.

The results of these optimisations were apparently supercritical aerofoils exhibiting weakly shocked solutions and a considerable improvement in off-design performance, with optimum values of Mach just below the design Mach objective [36].

Due to the higher robustness of range-based optimisation and its lower computational cost when compared to multi-point optimisation, the de Breguet range parameter (including an induced drag term) has been chosen as the desired objective function for the problem proposed. Most fuel is consumed during cruise for a typical airliner mission [37], so cruise optimisation has been selected for best results. In order to obtain a reliable solution that would not jeopardise the performance of the aerofoil at other mission points, a high-load cruise condition has been set as the objective for this optimisation ($M = 0.76$ and $C_L = 0.45$). The resulting objective function can then be written as:

$$\begin{aligned} \text{maximise}: \quad & \frac{C_L}{C_D + \kappa C_L^2} \\ \text{subject to}: \quad & MC_L^2 = 0.26 \\ & 0.115 < \frac{t}{c} < 0.125 \end{aligned} \tag{12}$$

Where the geometric thickness constraint has been chosen to accommodate the target thickness requirement. Typical geometric constraints are also based on keeping a minimum internal volume or area, which tends to be a more structurally realistic option for later design stages.

The resulting aerofoil must be able to produce higher values of lift at disparate mission conditions. In order to filter out aerofoils from the working library, incapable of meeting this constraint the technology factor was calculated for a value of $C_L = 0.74$, and aerofoils unable to achieve this value were filtered out. Similarly, aerofoils with thickness too large or small with respect to the target thickness were discarded.

5.2 Optimisation schemes

Once the design space has been parameterised adequately, and the working optimisation problem has been formulated mathematically, a suitable optimiser must be chosen to interrogate the design space. Typical optimisation methods can be divided into gradient-based and global search.

Gradient-based optimisers use the objective function sensitivities (*i.e.* the gradients with respect to the design variables) to define the fastest search direction to minimise the objective function. They are therefore computationally cheaper but are bound to stop in a local minimum - typical remedies include starting the optimisation using different aerofoil shapes or inducing several modifications to the same initial shape [38].

To determine sensitivities, the Hessian matrix of the objective function must be built, which requires twice as many objective function evaluations as design variables when using a finite difference scheme. An alternative was formulated by Jameson [39, 40] based on control theory. Instead of calculating the Hessian, a solution to a set of adjoint flow equations can be solved to obtain the sensitivities. The cost of solving the adjoint equations is comparable to that of the flow equations (one solver evaluation), and so Jameson's method provides significant relief in computational cost.

Global optimisation methods use search agents to provide full coverage of the design space. They are hence more expensive but are likely to converge to a global minimum. Nonetheless, they require a number of flow solver evaluations several orders of magnitude larger than their gradient-based counterparts and are hence seldom used for ASO.

6 Preliminary results

Values of the Korn technology factor for the training library oscillated between 0.67 and 0.86, with over 80% of the aerofoils scoring above 0.8 as originally expected. Nearly 300 aerofoils were filtered out as they were unable to meet the specified lift coefficient or the drag divergence Mach calculation was not accurate enough to ensure robustness. Most high scoring aerofoils were supercritical in nature, with the NPL 9510 aerofoil scoring a highest 0.96 Korn factor - the result was successfully validated against Hall *et al.* [41] and Jenkins [42], and the aerofoil identified as a potential initial shape for the optimisation.

The six first modes extracted from the aerofoil library containing the 100 highest scoring aerofoils using SVD are shown in Figure 1. The modes seem to encompass relevant physical significance - the first mode can be related to the aerofoil camber, whilst the second mode shows analogy to the overall aerofoil thickness. The third mode provides the gradient variations that are required to represent the supercritical aerofoils. Higher modes are less intuitive and get increasingly sinusoidal, as they provide the more refined oscillations required to represent complex details of the aerofoil shapes.

Figure 2 shows an example of mesh deformation using RBFs. The mesh quality was appreciated to be maintained throughout the deformation by running the flow solver for the deformed mesh and a newly generated mesh, and comparing results.

7 Preliminary conclusions

Aerodynamic shape optimisation is a complex discipline that involves multiple stages. Selection of a robust shape parameterisation method is essential to obtain good coverage of the design space.

Deformative parameterisation schemes provide greater flexibility and decoupling from the initial aerofoil selection, but are harder to integrate at the design stages due to reduced physical significance of the design variables.

Deformative schemes also suppress the need to regenerate the CFD mesh for every evaluation of the flow solver, but are thus highly influenced by the mesh deformation scheme used. RBFs provide decoupling between surface and mesh deformations, and maintain mesh quality throughout deformations, which makes them a suitable candidate to implement when using deformative parameterisation schemes.

An adequate mathematical formulation of the optimisation problem and its constrains is essential to provide a realistic reflection of the physical problem. A suitable optimisation algorithm must be chosen to perform the optimisation - a gradient-based optimiser has been identified as a potential candidate due to the lower computational cost with respect to a global optimiser.

8 Future work

Groundwork has been laid to start the optimisation process. It remains an exercise to find a suitable optimisation algorithm to minimise the proposed objective function. SNOPT [43, 44], a gradient-based optimisation scheme based on sequential programming, has been discerned as a potential candidate and coupling with the existing code has been left as a task for future work.

Identification and comparison of alternative optimisation algorithms remains a substantial area of research. Alternative sequential programming schemes that make use of parallel programming (*e.g.* FSQP[45]) could prove enriching sources for comparison with the chosen algorithm. Likewise, the feasibility of using an agent-based optimisation method may as well be studied as an extension to this project by exploiting the parallelisation capabilities of the software developed.

References

[1] Hicks, R. M. and Henne, P. A., "Wing design by numerical optimization", *Journal of Aircraft*, vol. 15, no. 7, pp. 407–412, 1978. DOI: 10.2514/3.58379.

[2] Spalart, P. R. and Venkatakrishnan, V., "On the role and challenges of CFD in the aerospace industry", *The Aeronautical Journal*, vol. 120, no. 1223, pp. 209–232, 2016. DOI: 10.1017/aer.2015.10.

[3] Vanderplaats, G. N., "Numerical optimization techniques", in *Computer Aided Optimal Design: Structural and Mechanical Systems. NATO ASI Series (Series F: Computer and Systems Sciences)*, C. A. M. Soares, Ed., vol. 27, Berlin, Heidelberg: Springer, 1987, pp. 197–239. DOI: 10.1007/978-3-642-83051-8_5.

[4] Vanderplaats, G. N., *Multidiscipline design optimization*. Monterey, CA: Vanderplaats Research & Development, Inc., 2007.

[5] Skinner, S. and Zare-Behtash, H., "State-of-the-art in aerodynamic shape optimisation methods", *Applied Soft Computing*, vol. 62, pp. 933–962, 2018. DOI: https://doi.org/10.1016/j.asoc.2017.09.030.

[6] Buckley, H. P., Zhou, B. Y. and Zingg, D. W., "Airfoil optimization using practical aerodynamic design requirements", *Journal of Aircraft*, vol. 47, no. 5, pp. 1707–1719, 2010. DOI: 10.2514/1.C000256.

[7] Masters, D. A., Taylor, N. J., Rendall, T. C. S., Allen, C. B. and Poole, D. J., "Geometric comparison of aerofoil shape parameterization methods", *AIAA Journal*, vol. 55, no. 5, pp. 1575–1589, 2017. DOI: 10.2514/1.J054943.

[8] Chernukhin, O. and Zingg, D. W., "Multimodality and global optimization in aerodynamic design", *AIAA Journal*, vol. 51, no. 6, pp. 1342–1354, 2013. DOI: 10.2514/1.J051835.

[9] Slooff, J. W., Schmidt, W., Papailiou, K. D., Bucciantini, G, Van der Vooren, J, Ashill, P. R., Holst, T. L. and Boppe, C. W., "Technical status review on drag prediction and analysis from computational fluid dynamics: State of the art", Advisory Group for Aerospace Research and Development, AGARD Advisory Report 256, 1989.

[10] Mason, W. H., "Analytic models for technology integration in aircraft design", in *Aircraft Design, Systems and Operations Conference*. American Institute of Aeronautics and Astronautics, 1990. DOI: 10.2514/6.1990-3262.

[11] Harris, C. D., "NASA supercritical airfoils", National Aeronautics and Space Administration, NASA Technical Paper 2969, 1990.

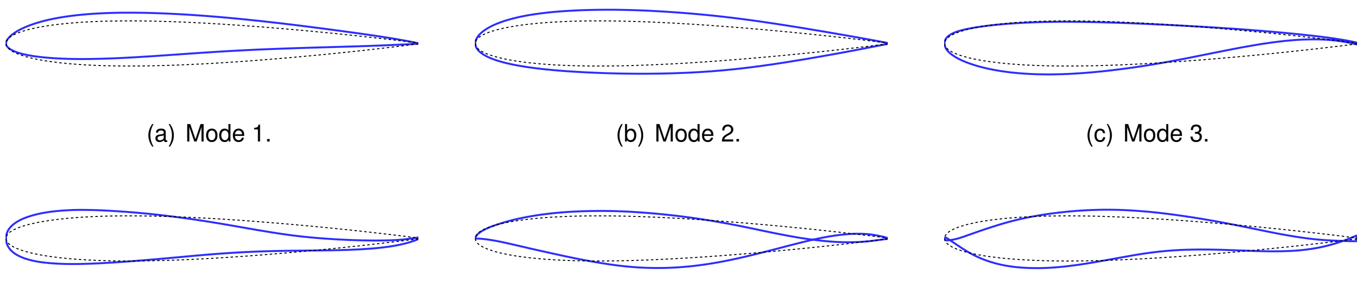

(a) Mode 1. (b) Mode 2. (c) Mode 3.

(d) Mode 4. (e) Mode 5. (f) Mode 6.

Figure 1: Extracted aerofoil library modes superimposed to NACA-0012 aerofoil.

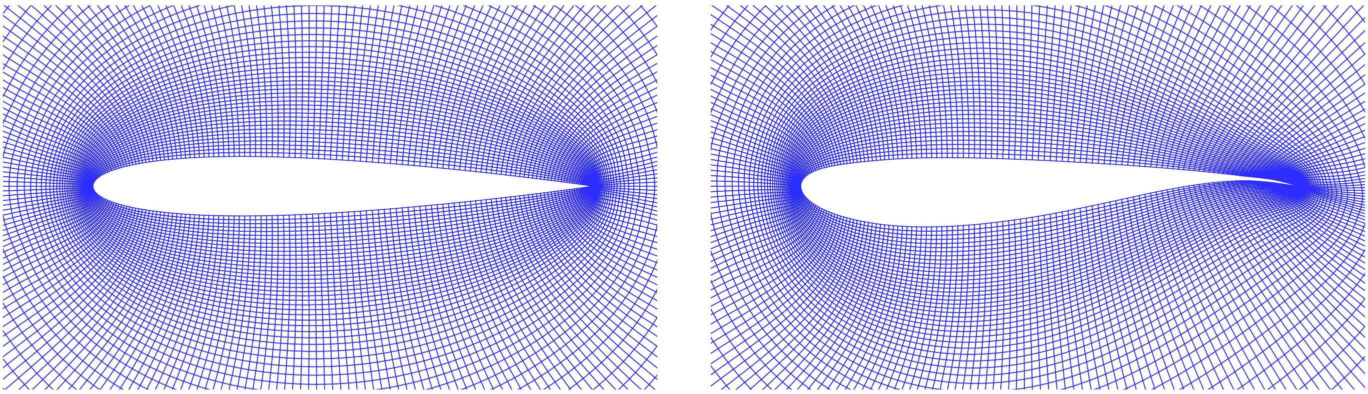

(a) Undeformed (NACA-0012). (b) Deformed (Mode 3).

Figure 2: 257×97 O-mesh used.

[12] Shevell, R. S., *Fundamentals of flight*, 2nd ed. Englewood Cliffs, N.J.: Prentice Hall, 1989.

[13] Anderson, J. D. J., *Fundamentals of aerodynamics*, 6th ed. New York, NY: McGraw-Hill Education, 2016.

[14] Golub, G. and Kahan, W., "Calculating the singular values and pseudo-inverse of a matrix", *Journal of the Society for Industrial and Applied Mathematics Series B Numerical Analysis*, vol. 2, no. 2, pp. 205–224, 1965. DOI: 10.1137/0702016.

[15] Leskovec, J., Rajaraman, A. and Ullman, J. D., "Dimensionality reduction", in *Mining of Massive Datasets*, 2nd ed. Cambridge University Press, 2014, pp. 384–414. DOI: 10.1017/CBO9781139924801.012.

[16] Poole, D. J., Allen, C. B. and Rendall, T. C. S., "Metric-based mathematical derivation of efficient airfoil design variables", *AIAA Journal*, vol. 53, no. 5, pp. 1349–1361, 2015. DOI: 10.2514/1.J053427.

[17] Batina, J. T., "Unsteady Euler airfoil solutions using unstructured dynamic meshes", *AIAA Journal*, vol. 28, no. 8, pp. 1381–1388, 1990. DOI: 10.2514/3.25229.

[18] Dwight, R. P., "Robust mesh deformation using the linear elasticity equations", in *Computational Fluid Dynamics 2006*, H. Deconinck and E. Dick, Eds., Berlin, Heidelberg: Springer Berlin Heidelberg, 2009, pp. 401–406.

[19] Wendland, H., *Scattered Data Approximation*, ser. Cambridge Monographs on Applied and Computational Mathematics. Cambridge University Press, 2004. DOI: 10.1017/CBO9780511617539.

[20] Buhmann, M. D., *Radial Basis Functions: Theory and Implementations*, ser. Cambridge Monographs on Applied and Computational Mathematics. Cambridge University Press, 2003. DOI: 10.1017/CBO9780511543241.

[21] Rendall, T. C. S. and Allen, C. B., "Unified fluid–structure interpolation and mesh motion using radial basis functions", *International Journal for Numerical Methods in Engineering*, vol. 74, no. 10, pp. 1519–1559, 2008. DOI: 10.1002/nme.2219.

[22] Morris, A. M., Allen, C. B. and Rendall, T. C. S., "CFD-based optimization of aerofoils using radial basis functions for domain element parameterization and mesh deformation", *International Journal for Numerical Methods in Fluids*, vol. 58, no. 8, pp. 827–860, 2008. DOI: 10.1002/fld.1769.

[23] Dereniowski, D. and Kubale, M., "Cholesky factorization of matrices in parallel and ranking of graphs", in *Parallel Processing and Applied Mathematics*, R. Wyrzykowski, J. Dongarra, M. Paprzycki and J. Waśniewski, Eds., Berlin, Heidelberg: Springer Berlin Heidelberg, 2004, pp. 985–992. DOI: 10.1007/978-3-540-24669-5_127.

[24] Allen, C. B. and Rendall, T. C. S., "CFD-based optimization of hovering rotors using radial basis functions for shape parameterization and mesh deformation", *Optimization and Engineering*, vol. 14, no. 1, pp. 97–118, 2013. DOI: 10.1007/s11081-011-9179-6.

[25] Morris, A. M., Allen, C. B. and Rendall, T. C. S., "Domain-element method for aerodynamic shape optimization applied to modern transport wing", *AIAA Journal*, vol. 47, no. 7, pp. 1647–1659, 2009. DOI: 10.2514/1.39382.

[26] Rendall, T. and Allen, C., "Efficient mesh motion using radial basis functions with data reduction algorithms", *Journal of Computational Physics*, vol. 228, no. 17, pp. 6231–6249, 2009. DOI: 10.1016/j.jcp.2009.05.013.

[27] Kulfan, B. and Bussoletti, J., "Fundamental parameteric geometry representations for aircraft component shapes", in *11th AIAA/ISSMO Multidisciplinary Analysis and Optimization Conference*. American Institute of Aeronautics and Astronautics, 2006. DOI: 10.2514/6.2006-6948.

[28] Kulfan, B., "A universal parametric geometry representation method - CST", in *45th AIAA Aerospace Sciences Meeting and Exhibit*. American Institute of Aeronautics and Astronautics, 2007. DOI: 10.2514/6.2007-62.

[29] Kulfan, B., "Modification of CST airfoil representation methodology", Unpublished

note, [Online]. Available: http://www.brendakulfan.com/docs/CST8.pdf.

[30] Zingg, D. and Billing, L., "Toward practical aerodynamic design through numerical optimization", in *18th AIAA Computational Fluid Dynamics Conference*. American Institute of Aeronautics and Astronautics, 2007. DOI: 10.2514/6.2007-3950.

[31] Buckley, H. P. and Zingg, D. W., "Approach to aerodynamic design through numerical optimization", *AIAA Journal*, vol. 51, no. 8, pp. 1972–1981, 2013. DOI: 10.2514/1.J052268.

[32] Morawetz, C. S., "On the non-existence of continuous transonic flows past profiles I", *Communications on Pure and Applied Mathematics*, vol. 9, no. 1, pp. 45–68, 1956. DOI: 10.1002/cpa.3160090104.

[33] Morawetz, C. S., "On the non-existence of continuous transonic flows past profiles II", *Communications on Pure and Applied Mathematics*, vol. 10, no. 1, pp. 107–131, 1957. DOI: 10.1002/cpa.3160100105.

[34] Morawetz, C. S., "On the non-existence of continuous transonic flows past profiles III", *Communications on Pure and Applied Mathematics*, vol. 11, no. 1, pp. 129–144, 1958. DOI: 10.1002/cpa.3160110107.

[35] Poole, D. J., Allen, C. B. and Rendall, T. C. S., "Objective function and constraints for robust transonic aerofoil optimization", in *58th AIAA/ASCE/AHS/ASC Structures, Structural Dynamics, and Materials Conference*, 2017. DOI: 10.2514/6.2017-0360.

[36] Poole, D. J., Allen, C. B. and Rendall, T. C. S., "Comparison of point design and range-based objectives for transonic aerofoil optimization", *AIAA Journal*, vol. 56, no. 8, pp. 3240–3256, 2018. DOI: 10.2514/1.J056627.

[37] Roberson, W., Root, R. and Adams, D., "Fuel conservation strategies: Cruise flight", *Boeing Aeromagazine*, no. QTR_04, 2007.

[38] Yu, Y., Lyu, Z., Xu, Z. and Martins, J. R., "On the influence of optimization algorithm and initial design on wing aerodynamic shape optimization", *Aerospace Science and Technology*, vol. 75, pp. 183 –199, 2018. DOI: 10.1016/j.ast.2018.01.016.

[39] Jameson, A., "Aerodynamic design via control theory", in *Recent Advances in Computational Fluid Dynamics*, C. C. Chao, S. A. Orszag and W. Shyy, Eds., Berlin, Heidelberg: Springer Berlin Heidelberg, 1989, pp. 377–401. DOI: 10.1007/978-3-642-83733-3_14.

[40] Jameson, A., "Aerodynamic shape optimization using the adjoint method", in *VKI Lecture Series on Aerodynamic Drag Prediction and Reduction, von Karman Institute of Fluid Dynamics, Rhode St Genese*, 2003.

[41] Hall, D. J., Quincey, V. G. and Lock, R. C., "Some results of wind-tunnel tests on an aerofoil section (NPL 9510) combining a 'peaky' upper surface-pressure distribution with rear loading", National Physics Laboratory, Tech. Rep. 1292, 1974.

[42] Jenkins, R. V., "Reynolds number tests of an NPL 9510 airfoil in the Langley 0.3-meter transonic cryogenic tunnel", *NASA Technical Memorandum*, Dec. 1983.

[43] Gill, P. E., Murray, W. and Saunders, M. A., "SNOPT: An SQP algorithm for large-scale constrained optimization", *SIAM Rev.*, vol. 47, pp. 99–131, 2005.

[44] Gill, P. E., Murray, W., Saunders, M. A. and Wong, E., "User's guide for SNOPT 7.7: Software for large-scale nonlinear programming", Department of Mathematics, University of California, San Diego, La Jolla, CA, Center for Computational Mathematics Report CCoM 18-1, 2018.

[45] Tits, A., Lawrence, C. and L. Zhou, J., "User's guide for CFSQP version 2.5: A C code for solving (large scale) constrained nonlinear (minimax) optimization problems, generating iterates satisfying all inequality constraints", *Technical report TR-94-16r1, University of Maryland, College Park*, Feb. 1999.

Workplan

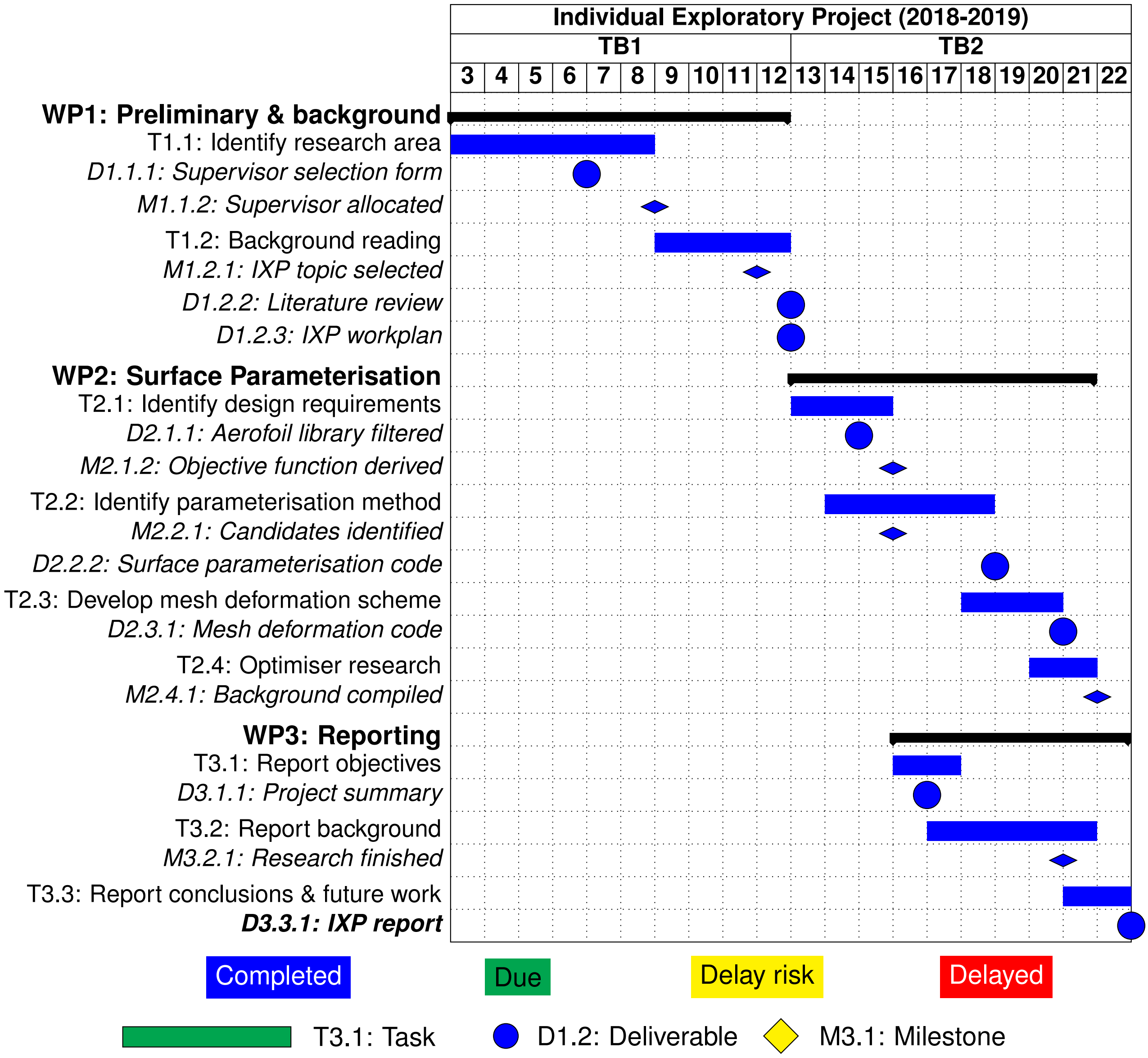

Figure 3: IXP planning and timescale.

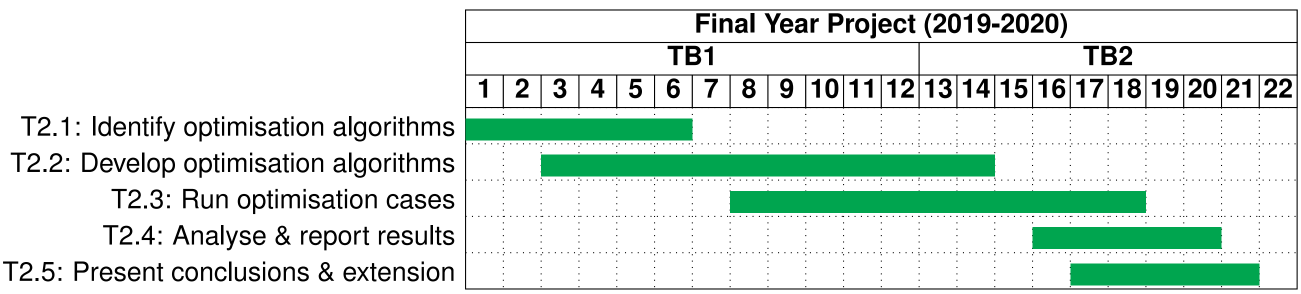

Figure 4: FYP planning and timescale.